Accepted Manuscript

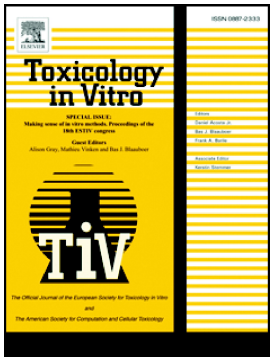

Phenylpropanoid-based sulfonamide promotes cyclin D1 and cyclin E down-regulation and induces cell cycle arrest at G1/S transition in estrogen positive MCF-7 cell line

Helloana Azevedo-Barbosa, Guilherme Álvaro Ferreira-Silva, Carolina Faria Silva, Thiago Belarmino de Souza, Danielle Ferreira Dias, Ana Claudia Chagas de Paula, Marisa Ionta, Diogo Teixeira Carvalho

PII: S0887-2333(18)30529-0
DOI: https://doi.org/10.1016/j.tiv.2019.04.023
Reference: TIV 4532

To appear in: *Toxicology in Vitro*

Received date: 4 September 2018
Revised date: 3 April 2019
Accepted date: 18 April 2019

Please cite this article as: H. Azevedo-Barbosa, G.Á. Ferreira-Silva, C.F. Silva, et al., Phenylpropanoid-based sulfonamide promotes cyclin D1 and cyclin E down-regulation and induces cell cycle arrest at G1/S transition in estrogen positive MCF-7 cell line, Toxicology in Vitro, https://doi.org/10.1016/j.tiv.2019.04.023

Phenylpropanoid-based sulfonamide promotes cyclin D1 and cyclin E down-regulation and induces cell cycle arrest at G1/S transition in estrogen positive MCF-7 cell line

Helloana Azevedo-Barbosa[a], Guilherme Álvaro Ferreira-Silva[b], Carolina Faria Silva[a], Thiago Belarmino de Souza[c], Danielle Ferreira Dias[d], Ana Claudia Chagas de Paula[e], Marisa Ionta[b,*] marisa.ionta@unifal-mg.edu.br, Diogo Teixeira Carvalho[a,*] diogo.carvalho@unifal-mg.edu.br

[a]LQFar - Laboratory of Research in Pharmaceutical Chemistry, Faculty of Pharmaceutical Sciences, Federal University of Alfenas, zip code 37130-001, Alfenas, MG, Brazil

[b]LabaInt - Laboratory of Integrative Animal Biology, Institute of Biomedical Sciences, Federal University of Alfenas, zip code 37130-001, Alfenas, MG, Brazil

[c]School of Pharmacy, Federal University of Ouro Preto, zip code 35400-000, Ouro Preto, MG, Brazil

[d]LFQM - Laboratory of Phytochemistry and Medicinal Chemistry, Institute of Chemistry, Federal University of Alfenas, zip code 37130-001, Alfenas, MG, Brazil

[e]Department of Pharmaceutical Sciences, College of Pharmacy, Federal University of Juiz de Fora, zip code 36036-900, Juiz de Fora, MG, Brazil

[*]Corresponding authors at: 700, Gabriel Monteiro da Silva Street, Zip code: 37130-001, Alfenas, MG, Brazil

Abstract

Cancer is one of the most critical problems of public health in the world and one of the main challenges for medicine. Different biological effects have been reported for sulfonamide-based compounds including antibacterial, antifungal, and antitumor activities. Herein, a series of phenylpropanoid-based sulfonamides (**4a**, **4a'**, **4b**, **4b'**, **5a**, **5a'**, **5b** and **5b'**) were synthesized and their cytotoxic activity was evaluated against four cell lines derived from human tumours (A549 – lung, MCF-7 – breast, Hep G2 - hepatocellular carcinoma, and HT-144-melanoma). Cell viability was significantly reduced in the MCF-7 cell line when compounds **4b**, **4b'** and **5a** were used; IC_{50} values were lower than those found for their precursors (eugenol and dihydroeugenol) and sulfanilamide. We observed that **4b** induced cell cycle arrest at G1/S transition. This is probably due to its ability to reduce cyclin D1 and cyclin E expression. Moreover, **4b** also induced apoptosis in MCF-7 cells as demonstrated by an increase in the cell population positive for annexin V in treated cultures in comparison to the control group. Taken together, the data showed that **4b** is a promising antitumor agent and it should be considered for further *in vivo* studies.

Keywords:

Phenylpropanoids; Sulfonamides; Molecular hybridization; Antiproliferative activity; Breast cancer.

1. Introduction

Cancer is the second major cause of death in the world population and breast cancer is the most frequent cancer in women worldwide (Torre et al., 2016). In 2012, about 1.67 million new cases of breast cancer were diagnosed, representing 25% of all cancers reported in women (Ferlay et al., 2015). Breast cancer is a heterogeneous disease characterized by a wide spectrum of clinical, pathological, and molecular features (Perou et al., 2000; Sorlie et al., 2003). Histologically, breast cancer has been classified into *in situ* carcinoma (cancer cells are confined to the pre-existing normal lobules or ducts) and invasive carcinoma (cancer cells invade the surrounding stroma) with their respective subdivisions (Malhotra et al., 2010). According to the gene expression profile, breast cancer has been classified as luminal A/B (estrogen and progesterone receptors positive); HER2-enriched (HER+) (amplification and/or overexpressing of human epidermal growth factor type 2 gene; basal-like (also known as triple negative once the majority of these tumours do not express ER, PR, or HER2); claudin-low (emerged from basal-like subtype, but display expression of claudins 3/4/7); and normal breast-like (Perou et al., 2000; Sorlie et al., 2003). Invasive carcinoma is the most common subtype (70-80%) diagnosed, and luminal A/B tumour subtypes are ER-positive corresponding to 40% of cases (Prat and Perou, 2011; Prat et al., 2015). The recognition of the tumour subtype at histological and molecular levels is essential for the choice of a more adequate therapy (Ross et al., 2008; Maughan et al., 2010).

Various anticancer drugs have been introduced in chemotherapeutic protocols, however many patients are refractory to currently available chemotherapy (Weir et al., 2011). Therefore, it is relevant to identify new substances with anticancer activity to overcome chemotherapy resistance.

Sulfonamides are classically known for being the central core in the structures of many antibacterial synthetic drugs such as sulfanilamide (4-aminobenzenesulfonamide, Scheme 1), a precursor substance of the class of sulfonamidic antibacterials (Lesch, 2007; Wainwright and Kristiansen, 2011). On the other hand, various bioactive molecules possessing the sulfonamide group exhibit potential antifungal (Wang et al., 2010), anti-inflammatory (Chen et al., 2005), antiviral (Supuran et al., 2004), antihypertensive (Kanda et al., 2001), diuretic (Neff and Nawarskas, 2010), hypoglycemic (Boyd, 1988), anticonvulsive (Parker et al., 2009), and hypolipemic (Takahashi et al., 2010) activity. In

addition, recent reports have demonstrated the antitumor potential of sulfonamide compounds. Despite the variety of structural patterns of these compounds, it has been demonstrated that the sulfonamide group is critical for their cytotoxic activity against cancer cell lines (Kamal et al., 2011; Fortin et al., 2011; Lal et al., 2013; Facchinetti et al., 2014; Kwon et al., 2015; Ghorab et al., 2015).

Eugenol (4-allyl-2-methoxyphenol, **1**, Scheme 1) is a natural allylphenol found in essential oils of many aromatic plants, such as cloves (*Syzygium aromaticum*), sassafras (*Ocotea odorifera*), and cinnamon (*Cinnamomum zeylanicum*) (Baskaran et al., 2010). Pharmacological activity of eugenol has been reported, especially relating to antibacterial and antifungal activities (Ahmad et al., 2010; Devi et al., 2010; Carrasco et al., 2012; Cortés-Rojas et al., 2014; Li et al., 2015). We have previously demonstrated that synthetic compounds obtained from natural phenylpropanoids have important antimicrobial activity (Souza et al., 2014; Souza et al., 2015; Abrão et al., 2015; Souza et al., 2016). There are several reports of anticancer properties of eugenol due to its ability to induce apoptosis in breast cancer cells (Al-Sharif et al., 2013; Júnior et al., 2016), leukaemia cells (Yoo et al., 2005), melanoma cells (Ghosh et al., 2005; Kim et al., 2006; Pisano et al., 2007), osteosarcoma cells (Shin et al., 2007), and prostate cancer cells (Ghosh et al., 2009). Furthermore, Manikandan et al. (2011) demonstrated the antitumor potential of eugenol against gastric carcinoma due to its ability to inhibit the angiogenesis process.

Molecular hybridization is a fairly new concept in drug design and its development is based on the combination of pharmacophoric moieties of different natural bioactive or synthetic substances to produce a new hybrid compound with improved affinity and efficacy when compared to the parent drugs (Viegas-Junior et al., 2007; Abbot et al., 2017). In the present study, we describe the synthesis of new sulfonamides prepared from eugenol (**4a**, **4a'**, **5a**, **5a'**) or dihydroeugenol (**4b**, **4b'**, **5b**, **5b'**) and the investigation of their cytotoxic potential against different cancer cell lines (A549, HepG2, HT-144 and MCF-7). The structural pattern of compounds was designed by molecular hybridization between the phenylpropanoid and sulfonamide subunit from sulfanilamide (Scheme 1). Furthermore, we evaluated the molecular mechanism underlying the cytotoxic activity of the compound **4b** on MCF-7 cells.

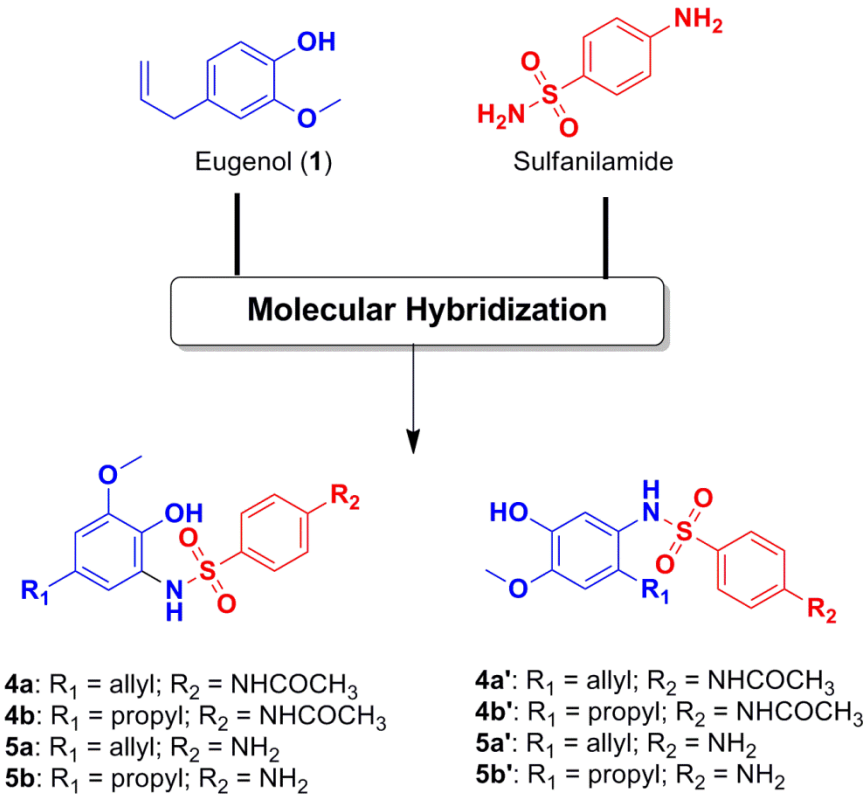

Scheme 1. Design of the new phenylpropanoid-based sulfonamides derivatives (**4a**, **4a'**, **4b**, **4b'**, **5a**, **5a'**, **5b** and **5b'**).

2. Results and Discussion

2.1 Synthesis and characterization of sulfonamide derivatives

The synthetic route used to obtain the molecular hybrids is depicted in Scheme 2.

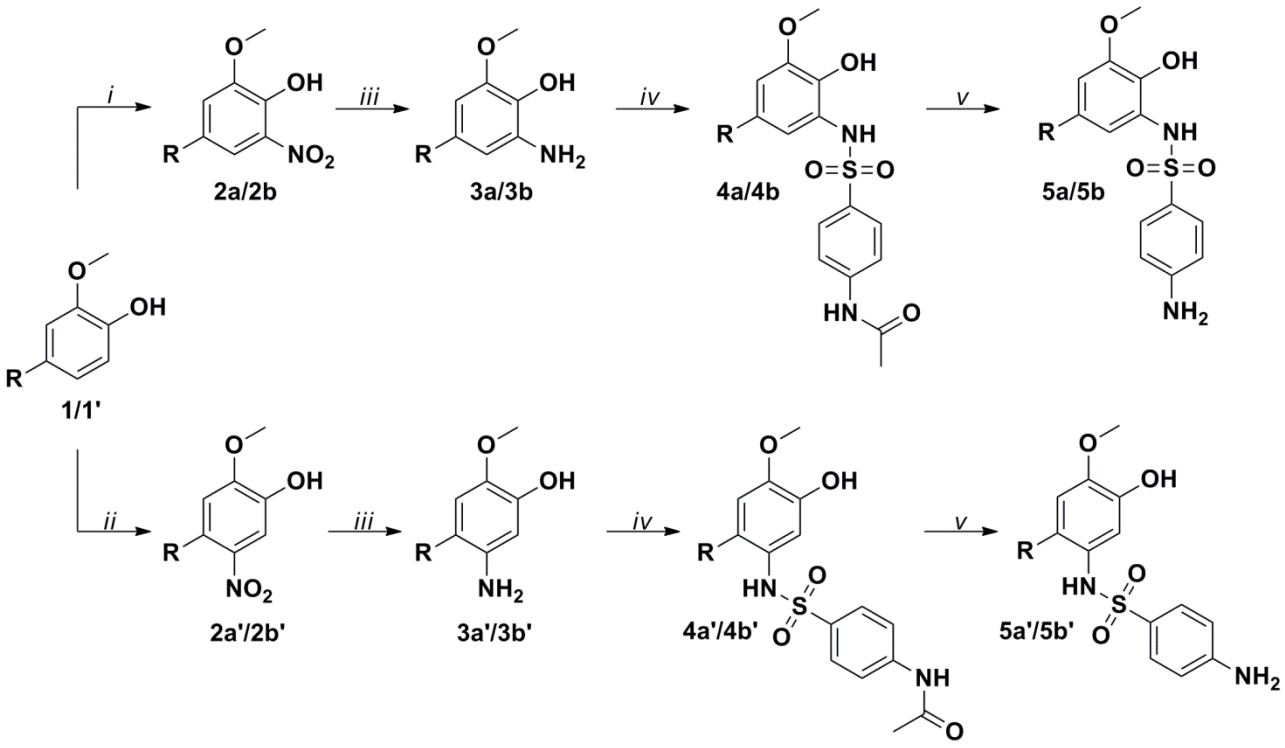

1, **2a**, **2a'**, **3a**, **3a'**, **4a**, **4a'**, **5a** and **5a'**: R = CH_2=CH-CH_2-
1', **2b**, **2b'**, **3b**, **3b'**, **4b**, **4b'**, **5b** and **5b'**: R = CH_3-CH_2-CH_2-

Scheme 2. Synthetic route to phenylpropanoid-based sulfonamide derivatives: *i)* $NaNO_3$, $KHSO_4$, SiO_2/H_2O (1:1), CH_2Cl_2, r.t.; *ii)* $Bi(NO_3)_3.5H_2O$, SiO_2, $CHCl_3$, 70 °C; *iii)* $SnCl_2.2H_2O$, EtOH, 80 °C; *iv)* 4-acetamidobenzenesulfonyl chloride, pyridine, 100 °C; *v)* $SOCl_2$, MeOH, r.t.

The synthesis of the desired compounds was achieved initially by nitration of eugenol (**1**) and dihydroeugenol (**1'**) under mild reaction conditions as described by Zolfigol et al. (2001) and Canales et al. (2011), who obtained *ortho*-nitrophenols and *meta*-nitrophenols, respectively, with high regioselectivity. The next step consisted of reducing these nitrated intermediates **2a**, **2b**, **2a'** and **2b'** with stannous chloride in ethanol (Belamy and Ou, 1984). The amphoteric aminophenol derivatives **3a**, **3b**, **3a'** and **3b'** were obtained as solids after careful acid-base extractions. The spectrometric data of nitro and amino intermediates showed perfect agreement with the expected ones. Subsequently, these aminophenols were converted to the respective 4-acetamidobenzenesulfonamides **4a**, **4b**, **4a'** and **4b'** by reaction with 4-acetamidobenzenesulfonyl chloride in refluxing pyridine (Silva et al., 2015). The identities of these compounds were confirmed by some key signals in their NMR spectra such as the sulfonamide NH in the range 8.95-8.74 ppm, the presence of a *para*-disubstituted aromatic ring-pattern, and the acetamide CH_3 at 2.05 ppm. Finally, the final sulfonamides (**5a**, **5b**, **5a'** and **5b'**) were obtained by deacetylation of 4-acetamidobenzenesulfonamides with thionyl chloride in methanol (Wang et al., 2012).

These products were obtained after preparative TLC for structural characterization and desired biological evaluations. NMR and IV spectra did not show the characteristic signals of the acetamidic group. In addition, it was possible to detect the presence of the typical aniline amino groups in the region of 8.6 and 8.4 ppm. The eight sulfonamides are undescribed substances and were fully characterized by IR, NMR, and HRMS analysis.

2.2 Biological assays

The synthetized compounds (**4a**, **4b**, **4a'**, **4b'**, **5a**, **5b**, **5a'** and **5b'**) were tested at 125 µM against four tumour cell lines derived from human tumours (A549, HT-144, HepG2 and MCF-7). The concentration used in pre-screening was determined in a previous pilot study (data not known). We observed a significant reduction in viability only in MCF-7 cultures treated with **4b**, **4b'** and **5a** compounds (Fig. 1A). Thus, MCF-7 cells were selected to determine IC_{50} values of these molecules (Table 1 and Fig.1B). We found that **4b**, **4b'** and **5a** were more cytotoxic than their precursors (eugenol and dihydroeugenol) or sulfanilamide. IC_{50} values of eugenol and dihydroeugenol were upward to 1,500 µM, while IC_{50} values of **4b**, **4b'** and **5a** were, respectively,133.80 ± 2.36 µM, 116.60 ± 1.83 µM and 164.90 ± 6.13 µM. Therefore **4b**, **4b'**, and **5a** were potentially more efficient in reducing the viability of MCF-7 cells (more than 10-fold) in relation to their precursors.

The cytotoxic potential of **4b**, **4b'**, and **5a** on MCF-7 cells may be related to the propyl side chain and acetamide group, because **4b** and **4b'** were more active than their allylic analogues **4a** and **4a'** or even those with the free arylamine group, **5b** and **5b'**.The *ortho* position of the sulfonamide group in relation to the phenolic hydroxyl seems to also contribute to the observed activity profile since the analogues **4a'**, **4b'**, **5a'**, and **5b'**, that present the sulfonamide group *meta* in relation to the hydroxyl phenol, were less active.

We also sought to investigate the cytotoxic profile of **4b**, **4b'**, and **5a** on normal cells, an important aspect for the development of therapeutic drugs. For this purpose, we performed dose-response curves using fibroblasts derived from human normal skin (CCD-1059Sk), and non-transformed breast epithelial cells (MCF 10A). We could observe a lower cytotoxicity of **4b**, **4b',** and **5a** on normal cells when compared to tumour cells (Fig. 1C). Thus, these compounds seem to have selectivity toward MCF-7 cells.

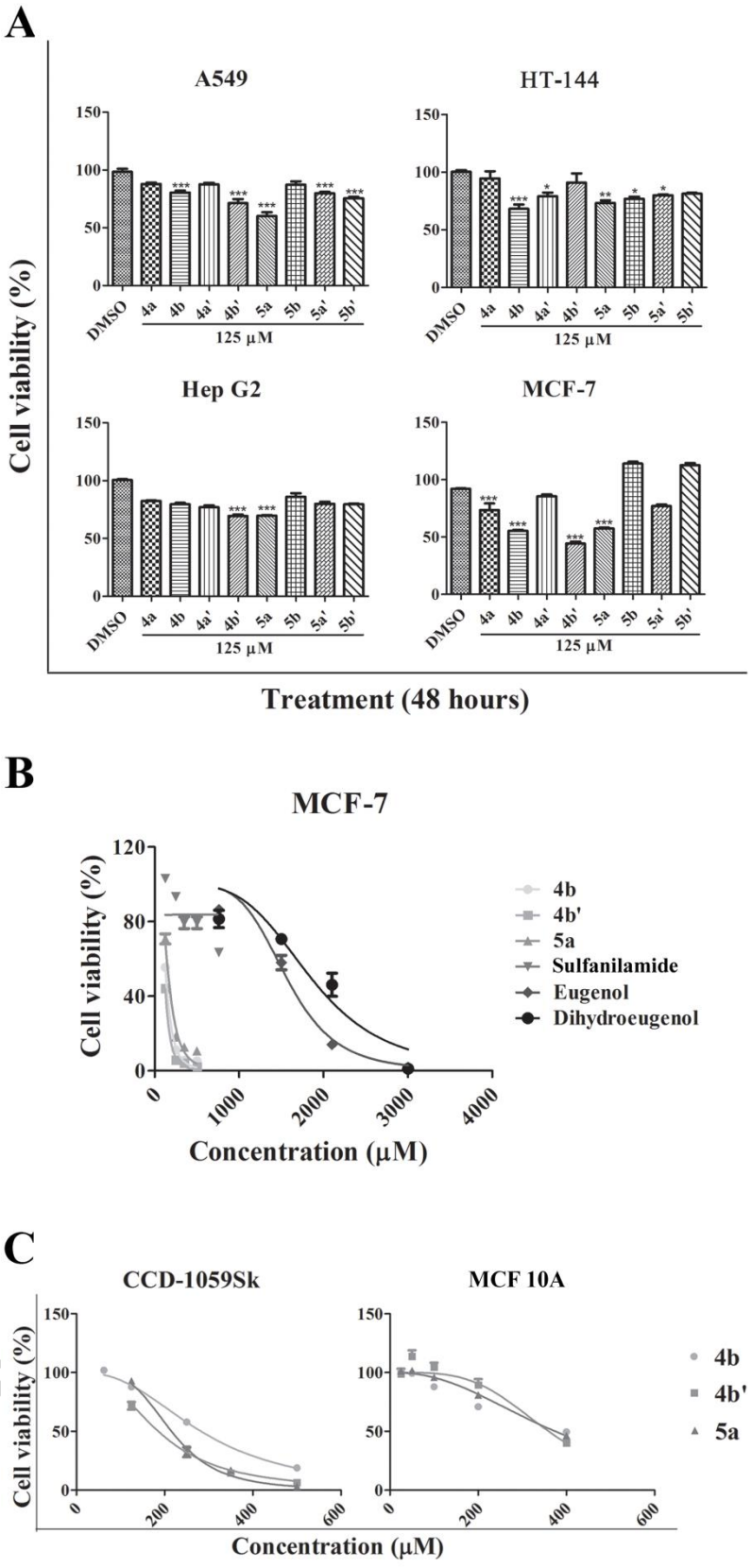

Fig.1. Cell viability determined by rezasurin assay. (A) Cells were treated with different molecules at 125 µM for 48 h. (B) Dose response curves determined after 48 h of treatment with **4b**, **4b', 5a,** and their precursors (sulfanilamide, eugenol and dihydroeugenol) in MCF-7 cells. (C) Dose response curves determined after 48 h of treatment with **4b**, **4b'**, and **5a** in normal cells. Significant differences from control groups were determined according to ANOVA followed by Tukey's post-test from three independent experiments.*** $p < 0.001$, ** $p < 0.01$, and * $p < 0.05$.

Table 1. IC_{50} values (μM) determined after 48 of treatment with the compounds **4b**, **4b'**, **5a**, and their precursors.

Compounds	IC_{50} ± Standard Deviation			
	MCF-7	CCD-1059Sk	MCF10A	
4b	133.80 ± 2.36	282.80 ± 5.11	> 300	
4b'	116.60 ± 1.83	185.90 ± 5.04	> 300	
5a	164.90 ± 6.13	215.80 ± 6.79	> 300	
Eugenol	> 1500.00	-	-	
Dihydroeugenol	> 1500.00	-	-	
Sulfanilamide	> 1000.00	-	-	

We selected **4b** for further studies to understand better the effect of this substance on MCF-7 cells. We investigated the proliferative behaviour of MCF-7 cells treated with **4b** through different methodological approaches**.** The morphological features of the MCF-7 cells after treatment with **4b** are shown in Fig. 2A. Large cells were observed in cultures treated with **4b** at 50 μM. While small and rounded cells were frequently observed in cultures treated with **4b** at 100 μM or 200 μM. This indicates cell detachment from the substrate, similar to the process observed in cell death (Fig. 2A). In addition, it was possible to observe cell density reduced in all treated samples compared to untreated cultures (Fig. 2A). The colonies number was also reduced in samples treated with **4b** at 50 or 100 μM in comparison to control samples, and **4b** at 200 μM had high cytotoxic activity on MCF-7 cells inhibiting completely the colony formation (Fig. 2B).

We observed a drastic reduction of viable cells in samples treated for 48 h and 72 h when compared to control groups (Fig. 2C). Furthermore, we demonstrated that **4b** reduced the frequency of mitosis and the clonogenic capacity of MFC-7 cells (Figs. 2B and 2D). The quantification of the different phases of mitosis showed that, with exception of prophase, all other sub-phases of the mitosis were drastically reduced in samples treated with **4b** at 100 μM (Fig. 2E). Therefore, taken together, the data showed that **4b** effectively inhibited the proliferation of MCF-7 cells.

DNA quantification was performed by flow cytometry to investigate the possible influence of **4b** compounds on cell cycle progression of MCF-7 cells. The dynamic of progression of the cell cycle was altered after 48 h treatment (Fig. 3A and 3B). Cultures treated with **4b** exhibited a G0/G1 population increase ($p < 0.001$), while S- and G2/M-populations were decreased ($p < 0.05$) when compared to control groups, indicating G1/S arrest. This finding is very promising considering that human cancers commonly show a deregulated control of G1 phase progression (Kumari et al., 2016).

Unfortunately, we could not compare our results concerning cell cycle progression with the literature, considering that **4b** represents an innovative chemical structural pattern. However, it has been reported that eugenol and isoeugenol modulated the expression profile of important regulators of cell cycle at G1/S transition, including RB protein (retinoblastoma protein), CDK6 (cyclin-dependent kinase 6), and p27(KIP1) in normal keratinocytes (Kalmes and Blömeke, 2012). In addition, the sulfonamide compounds synthesized by Kamal et al. (2011) induced G0/G1 cell cycle arrest in the K562 leukaemia cell line.

Cell cycle regulation at G1 progression and G1/S transition involve activation of protein complexes such as cyclin D-CDK4/6 and cyclin E-CDK2 (Matsuura et al., 2004). These complexes are responsible for RB phosphorylating, a tumour suppressor protein. Hyperphosphorylated RB dissociates from the E2F (transcription factor) that promotes the transcription of important genes for S phase (Foster et al., 2010).

In the present study, we investigated the influence of **4b** on cyclin D1 and cyclin E expression. The results showed that **4b** reduced expression levels of cyclin D1 in samples treated with 100 µM and cyclin E in samples treated with both 50 and 100 µM (Fig. 3C). Cyclin E is a critical regulator of G1/S transition and we associated the reduction in cyclin E expression levels induced by **4b** to the increase in the G1-cell population**.** Our findings are promising because cyclins D and E are commonly overexpressed in breast cancer and they are closed related to breast tumour progression (Kim and Diehl, 2009; Davis et al., 2014).

Finally, we verified whether the increased sub-G1 population observed by flow cytometry was related to apoptosis induction. We frequently observed in cytological preparation cells with condensed chromatin (Fig. 4A) similarly to cells in early stage of apoptosis (Yang et al., 2015). Thus, we performed an Annexin V assay and assessed mitochondria integrity using MitoTracker® Red fluorescent dye. There was a significant increase in cell population positive for Annexin V in samples with 50 and 100 µM, demonstrating pro-apoptotic activity of **4b** on MCF-7 cells (Fig. 4B). Interestingly, we found a cell population less labelled to MitoTracker® Red in samples treated with **4b** at 100 µM (Fig. 4C) reinforcing pro-apoptotic activity of this substance (Cottet-Rousselle et al., 2011). The resistance to apoptosis is a hallmark of cancer cells (Hanahan and Weinberg, 2011), and apoptosis evasion drastically contributes to resistance both to cancer treatments and tumour progression.

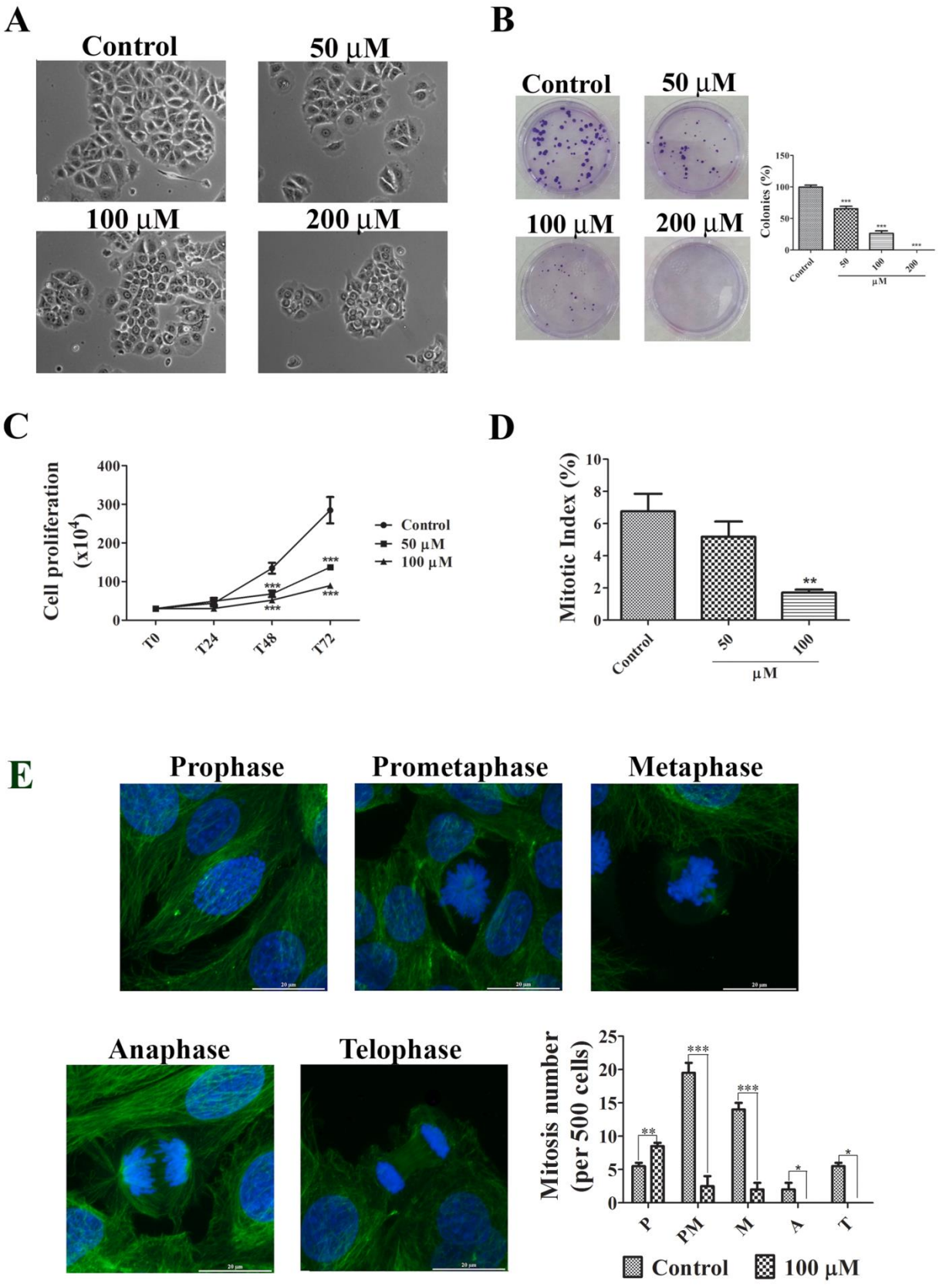

Fig. 2. Effect of **4b** on proliferative behaviour of MCF7**.** (A) Representative images obtained by phase contrast microscopy (60× magnification) showing morphological features of MCF-7 cells treated with **4b** or vehicle (DMSO) for 48 h. (B) Illustrative images and quantitative analysis of clonogenic capacity assay. (C) Cell proliferation determined by trypan blue exclusion assay after 24, 48, and 72 h of treatment with **4b**. (D)

Mitotic indexes determined from cytological preparations stained with DAPI and anti-α-tubulin. The pattern of staining is shown in (E) that also shows quantitative analysis of the different stages of mitosis after 48 h of treatment. Cells in anaphase and telophase were not observed in treated samples. Significant differences from control groups were determined using ANOVA followed by Tukey's post-test from three independent experiments. *$p < 0.05$, **$p < 0.01$, and ***$p < 0.001$

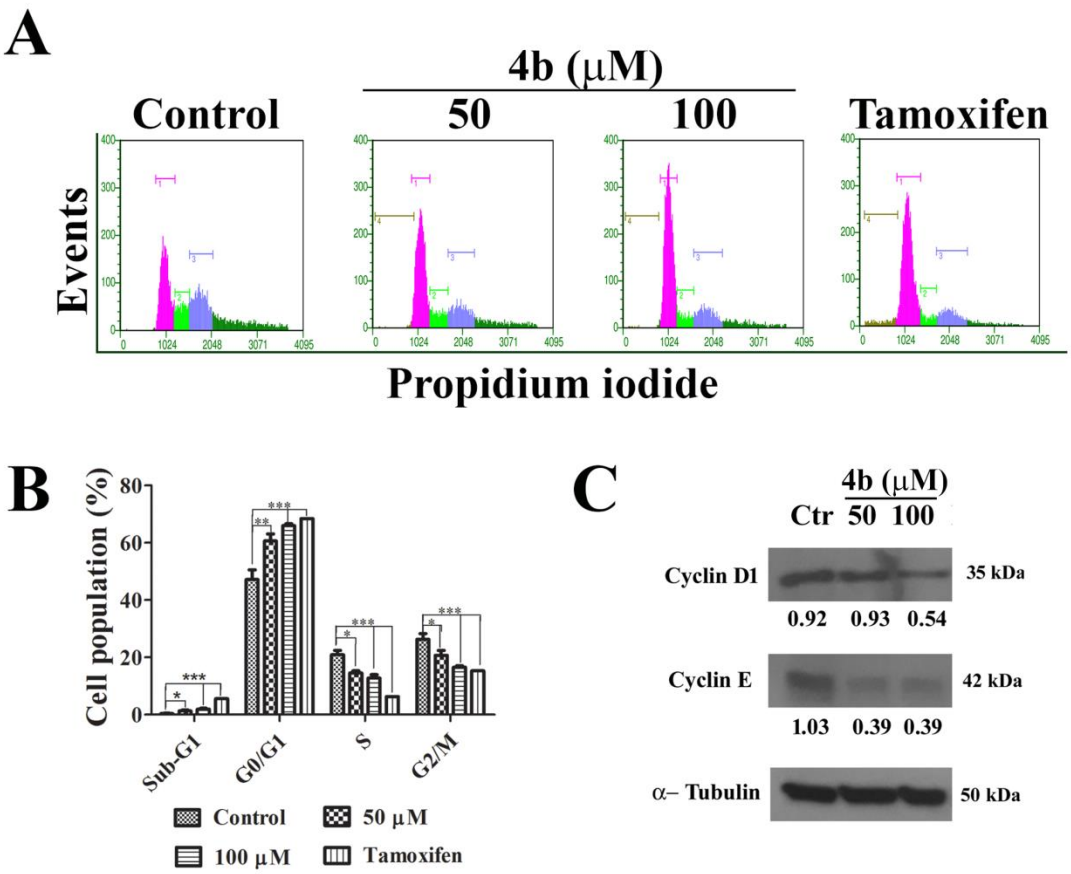

Fig. 3. Cell cycle analyses. (A) Illustrative histograms showing cell populations distributed in different phases of the cell cycle after 48 h of treatment with **4b**. Tamoxifen was used as a positive control at 25 μM. (B) Cell cycle analysis. Brown, pink, green, and blue bars represent, respectively, Sub-G1, G0/G1, S, and G2/M phases. (C) Cyclin D1 and cyclin E expression profiles were determined by western blot. α-tubulin was used as a loading control. Significant differences from control groups were determined using ANOVA followed by Tukey's post-test from three independent experiments. *$p < 0.05$, **$p < 0.01$, and ***$p < 0.001$

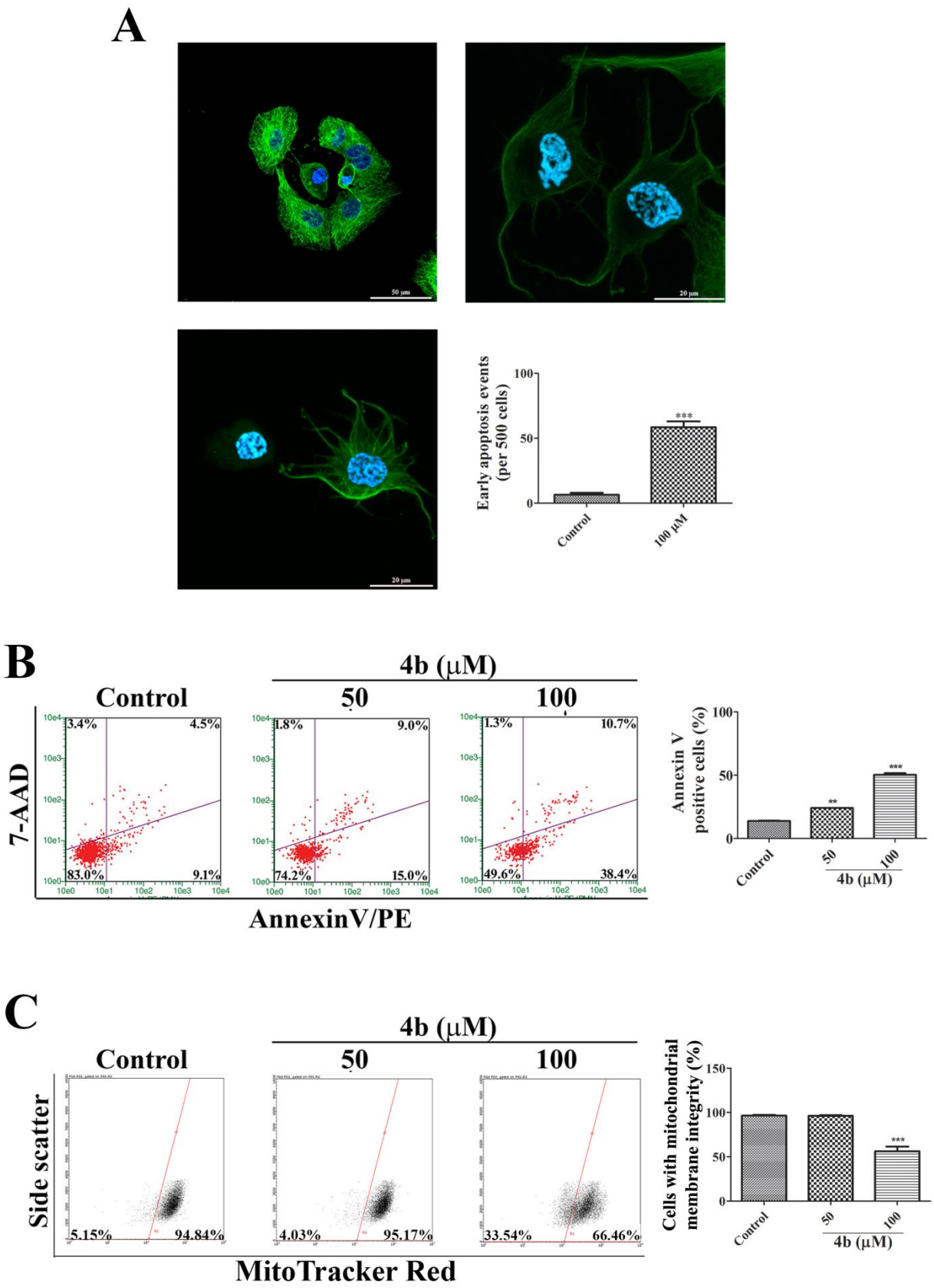

Fig.4. Pro-apoptotic analyses. (A) Fluorescent images from cell cultures treated at 100 µM with **4b** showing cells with condensed chromatin (green: microtubule network and blue: nuclei). (B) Annexin V-PE/7-AAD assay. Viable cells: lower left quadrants; early apoptotic cells: lower right quadrants; late apoptotic cells: upper right quadrants; necrotic cells: upper left quadrants. (C) Viable cells with intact mitochondrial

membrane (to the right from red line), and cells with loss of the mitochondrial integrity (to the left from red line). Significant differences from control groups were determined using ANOVA followed by Tukey's post-test from three independent experiments. $^{**}p < 0.01$ and $^{***}p < 0.001$

3. Conclusion

A phenylpropanoid-sulfonamide hybrid (**4b**) has an innovative structural scaffold and displays promising antitumor activity against MCF-7 cells. We demonstrated that this substance reduced cyclin D1 and cyclin E expression in MCF-7 cells, leading to cell cycle arrest in G1/S transition, and subsequently, apoptosis. Taken together, these findings demonstrate that **4b** should be considered for further *in vivo* studies to validate its antitumor activity against positive estrogen receptor breast cancer.

4. Material and methods

4.1 Materials and instrumentation

Eugenol and dihydroeugenol were purchased from Sigma (São Paulo, Brazil) and were used as such. Thin-layer chromatography (TLC) on silica gel-G plates (Macherey-Nagel, DC-Fertigfolien ALUGRAM® Xtra Sil G/UV_{254}) was used to monitor reactions courses. For column chromatography, column grade silica gel (Sorbiline; 0.040-0.063mm mesh size) was employed. Melting points of the compounds were obtained on a Bücher 535 melting-point apparatus and are uncorrected. IR spectra were recorded on a Shimadzu FTIR-Affinity-1. NMR spectra were recorded on a Bruker AC-300 spectrometer (Rheinstetten, Germany) (300 MHz for ^{1}H-NMR and 75 MHz for ^{13}C-NMR spectra) in deuterated chloroform or dimethylsulfoxide. Chemical shifts (δ) were reported in parts per million (ppm) with reference to tetramethylsilane (TMS) as internal standard and coupling constants (*J*) were reported in Hertz (Hz). High resolution mass (HRMS) spectra were obtained on a quadrupole time-of-flight instrument (Waters Xevo G2-S QTOF, Massachusetts, U.S.A), equipped with an ESI positive and negative ion source.

4.2 Synthesis of phenylpropanoid-based sulfonamide derivatives

4.2.1 Synthesis of nitro derivatives 2a and 2a'

To a solution of eugenol (**1**, 32.53 mmol) or dihydroeugenol (**1'**, 31.26 mmol) in dichloromethane (50 mL) were added equimolar amounts of sodium bisulfate and potassium nitrate, followed by addition of wet silica gel (1:1 w/w; 6.5 g for eugenol reaction and 6.3 g for dihydroeugenol reaction). The reaction was kept under vigorous magnetic stirring at room temperature for 48 h and monitored by TLC (chloroform/methanol, 9.5:0.5, v/v). After completion of the reaction, the mixture was filtered off, the filtrate was dried over anhydrous sodium sulfate and concentrated under reduced pressure. The nitro compound was purified by column chromatography (silica gel, hexane/ethyl acetate, 9/1, v/v).

*4-allyl-2-methoxy-6-nitrophenol (**2a**)* Yellow oil; 47% yield; IR ($\bar{\upsilon}_{máx}$, in cm^{-1}): 3520 (O-H), 1600, 1550 (C=C), 1515, 1440 (NO_2), 1270 (C-O-C); ^{1}H NMR (δ ppm; $CDCl_3$; 300 MHz): 10.6 (s, 1H, O-H), 7.4 (d, 1H, H5, *J* = 1.8 Hz), 6.9 (d, 1H, H3, *J* = 1.8 Hz), 5.9-5.8 (m, 1H, CH_2=CH-CH_2), 5.1-5.0 (m, 2H, CH_2=CH-CH_2), 3.9 (s, 3H, OCH_3), 3.3 (d, 2H, CH_2=CH-CH_2, *J* = 6.6 Hz); ^{13}C NMR (δ ppm; $CDCl_3$; 75 MHz): 149.8 (C6), 144.8 (C1), 135.9 (CH_2=CH-CH_2), 133.5 (C2), 131.2 (C4), 118.5 (C5), 117.1 (CH_2=CH-CH_2), 115.0 (C3), 56.6 (OCH_3), 39.3 (CH_2=CH-CH_2).

*2-methoxy-6-nitro-4-propylphenol (**2a'**)* Yellow oil; 67% yield; IR ($\bar{\upsilon}_{máx}$, in cm^{-1}): 3250 (O-H), 1591 (C=C), 1541, 1448 (NO_2), 1260 (C-O-C); ^{1}H NMR (δ ppm; $CDCl_3$; 300 MHz): 10.6 (s, 1H, O-H), 7.4 (d, 1H, H5, *J* = 1.8 Hz), 6.9 (d, 1H, H3, *J* = 1.8 Hz), 3.9 (s, 3H, OCH_3), 2.5 (t, 2H, CH_3-CH_2-CH_2, *J* = 7.2 Hz), 1.7-1.5 (m, 2H, CH_3-CH_2-CH_2), 0.9 (t, 3H, CH_3-CH_2-CH_2, *J* = 7,2 Hz); ^{13}C NMR (δ ppm; $CDCl_3$; 75 MHz): 149.7 (C6), 144.5 (C1), 133.8 (C4), 133.6 (C2), 118.7 (C5), 114.8 (C3), 56.7 (OCH_3), 37.3 (CH_3-CH_2-CH_2), 24.1 (CH_3-CH_2-CH_2), 13.5 (CH_3-CH_2-CH_2).

4.2.2 Synthesis of nitro derivatives 2b and 2b'

To a suspension of bismuth nitrate pentahydrate (1 eq.) in chloroform (50 mL) were added eugenol (**1**, 32.53 mmol) or dihydroeugenol (**1'**, 31.26 mmol) and silica gel (8 eq.). The mixture was refluxed under stirring for 30 minutes and was monitored by TLC (chloroform/methanol, 9.5/0.5, v/v). The mixture was then filtered off, the filtrate was dried over anhydrous sodium sulfate and concentrated under reduced pressure. The nitro compound was purified by column chromatography (silica gel, hexane/ethyl acetate, 9/1, v/v).

*4-Allyl-2-methoxy-5-nitrophenol (**2b**):* Dark yellow oil; 42% yield; IR ($\bar{\upsilon}_{máx}$, in cm^{-1}): 3231 (O-H), 1601 (C=C), 1538, 1444 (NO_2), 1261 (C-O-C). ^{1}H-NMR (δ ppm; $CDCl_3$, 300 MHz): 10.65 (s, 1H, O-H), 7.52 (s, 1H, H6), 6.97 (s, 1H, H3), 5.96-5,87 (m, 1H, CH_2=CH-CH_2), 5.17-5.10 (m, 2H, CH_2=CH-CH_2), 3.94 (s, 3H, OCH_3), 3.37 (d, 2H, *J* = 5.0 Hz, CH_2=CH-CH_2). ^{13}C-NMR (δ ppm; $CDCl_3$, 75 MHz): 149.7 (C5), 145.0 (C1), 136.0 (CH_2=CH-CH_2), 133.0 (C2), 131.1 (C4), 118.6 (C6), 117.1 (CH_2=CH-CH_2), 115.1 (C3), 56.8 (OCH_3), 39.5 (CH_2=CH-CH_2).

*2-methoxy-5-nitro-4-propylphenol (**2b'**):* Yellow oil; 21% yield; IR ($\bar{\upsilon}_{máx}$, in cm^{-1}): 3221 (O-H), 1541, 1448 (NO_2), 1260 (C-O-C). ^{1}H-NMR (δ ppm; $CDCl_3$, 300 MHz): 10.62 (s, 1H, O-H), 7.49 (d, 1H, *J* = 2.0 Hz, H6), 6.96 (d, 1H, *J* = 1.8 Hz, H3), 3.93 (s, 3H, OCH_3), 2.58 (t, 2H, *J* = 7.5 Hz, CH_3-CH_2-CH_2), 1.70-1.58 (m, 2H, CH_3-CH_2-CH_2), 0.97 (t, 3H, *J* = 7.2 Hz, CH_3-CH_2-CH_2). ^{13}C-NMR (δ ppm; $CDCl_3$, 75 MHz): 149.8 (C5), 144.7 (C1), 133.9 (C2), 133.7 (C4), 118.8 (C6), 115.0 (C3), 56.8 (OCH_3), 37.5 (CH_3-CH_2-CH_2), 24.3 (CH_3-CH_2-CH_2), 13.7 (CH_3-CH_2-CH_2).

4.2.3 Synthesis of amino derivatives 3a, 3b, 3a' and 3b'

The nitro compound **2a**, **2b**, **2a'**, or **2b'** (1 eq.) was solubilized in ethanol (50 mL) and stannous chloride dihydrate (5 eq.) was added to this solution. The suspension was refluxed under magnetic stirring for 3 h and the consumption of starting material was followed by TLC (chloroform/methanol, 9.5/0.5, v/v). The mixture was allowed to cool down and then poured into ice water. The pH was then adjusted to 7-8 by aqueous 5% $NaHCO_3$. Then, the mixture was extracted with ethyl acetate (3 x 50 mL) and the organic layer was dried with anhydrous sodium sulfate, filtered, and the filtrate was concentrated under reduced pressure, which afforded the crude products. These were next purified by column chromatography (silica gel, hexane/ethyl acetate, 8/2, v/v).

*4-Allyl-2-amino-6-methoxyphenol (**3a**):* Light yellow solid; 60% yield; m.p.: 95-98 ºC; IR ($\bar{\upsilon}_{máx}$, in cm^{-1}): 3371, 3311, 3074, 1606, 1512, 1456, 1230. ^{1}H-NMR (δ ppm; $CDCl_3$, 300 MHz): 6.25 (d, 1H, *J* = 1.8 Hz), 6.19 (d, 1H, *J* = 1.8 Hz), 6.00-5.87 (m, 1H), 5.11-5.02 (m, 2H), 3.84 (s, 3H), 3.24 (d, 2H, *J* = 6.9 Hz). ^{13}C-NMR (δ ppm; $CDCl_3$, 75 MHz): 146.6 (C6), 137.9 (CH_2=CH-CH_2), 133.8 (C2), 131.7 (C4), 131.2 (C1), 115.3 (CH_2=CH-CH_2), 109.5 (C5), 102.0 (C3), 56.0 (OCH_3), 40.1 (CH_2=CH-CH_2).

*2-amino-6-methoxy-4-propylphenol (**3b**):* Light beige solid; 63% yield; m.p.: 63-66 ºC; IR ($\bar{\upsilon}_{máx}$, in cm^{-1}): 3370, 3307, 3012, 1513, 1212. ^{1}H-NMR (δ ppm; $CDCl_3$, 300 MHz): 6.24 (d, 1H, *J* = 1.8 Hz), 6.19 (d, 1H, *J* = 1.8 Hz), 3.85 (s, 3H), 2.45 (t, 2H, *J* = 7.2 Hz), 1.66-1.53 (m, 2H), 0.93 (t, 3H, *J* = 7.5 Hz). ^{13}C-NMR (δ ppm; $CDCl_3$, 75 MHz): 146.5 (C6), 134.4 (C2), 133.8 (C4), 130.9 (C1), 109.3 (C5), 101.8 (C3), 55.9 ($O\underline{C}H_3$), 38.0 (CH_3-CH_2-$\underline{C}H_2$), 24.7 (CH_3-$\underline{C}H_2$-CH_2), 13.8 ($\underline{C}H_3$-CH_2-CH_2).

*4-Allyl-5-amino-2-methoxyphenol (**3a'**):* Light orange solid; 60% yield; m.p.: 105-107 ºC. IR ($\bar{\upsilon}_{máx}$, in cm^{-1}): 3369, 3305, 3071, 1606, 1513, 1456, 1214. ^{1}H-NMR (δ ppm; $CDCl_3$, 300 MHz): 6.25 (d, 1H, *J* = 1.8 Hz), 6.20 (d, 1H, *J* = 1.7 Hz), 5.99-5.87 (m, 1H), 5.11-5.03 (m, 2H), 4.08 (s, 2H), 3.84 (s, 3H), 3.25 (d, 2H, *J* = 6.7 Hz). ^{13}C-NMR (δ ppm; $CDCl_3$, 75 MHz): 147.2 (C2), 138.5 (CH_2=$\underline{C}$H-CH_2), 133.8 (C5), 131.7 (C4), 131.2 (C1), 115.9 ($\underline{C}H_2$=CH-CH_2), 110.0 (C3), 102.4 (C6), 57.0 ($O\underline{C}H_3$), 40.7 (CH_2=CH-$\underline{C}H_2$).

*5-amino-2-methoxy-4-propylphenol (**3b'**):* Light beige solid; 19% yield; m.p.: 82-84 ºC. IR ($\bar{\upsilon}_{máx}$, in cm^{-1}): 3370, 3307, 3016, 1514, 1214. ^{1}H-NMR (δ ppm; $CDCl_3$, 300 MHz): 6.24 (d, 1H, *J* = 1.8 Hz), 6.19 (d, 1H, *J* = 1.8 Hz), 3.84 (s, 3H), 2.44 (t, 2H, *J* = 7.7 Hz), 1.66-1.53 (m, 2H), 0.93 (t, 3H, *J* = 7.3 Hz). ^{13}C-NMR (δ ppm; $CDCl_3$, 75 MHz): 146.5 (C2), 134.4 (C5), 133.8 (C4), 130.9 (C1), 109.3 (C3), 101.8 (C6), 55.9 ($O\underline{C}H_3$), 38.0 (CH_3-CH_2-$\underline{C}H_2$), 24.7 (CH_3-$\underline{C}H_2$-CH_2), 13.8 ($\underline{C}H_3$-CH_2-CH_2).

4.2.4 Synthesis of 4-acetamidobenzenesulfonamides 4a, 4b, 4a' and 4b'

The amino derivatives **3a**, **3b**, **3a'**, or **3b'** (1 eq.) and 4-acetamidobenzenesulfonyl chloride (1 eq.) were solubilized in pyridine (5 mL) and this mixture was refluxed for 3 h under vigorous stirring. The progress of the reaction was monitored by TLC (hexane/ethyl acetate, 6/4, v/v). The reaction mixture was allowed to cool down and then poured into ice water. The pH was adjusted to 1-2 with hydrochloric acid before being extracted with ethyl acetate (3 x 50 mL). The organic phase was dried over anhydrous sodium sulfate and concentrated under reduced pressure to afford the crude product which was purified by column chromatography (silica gel, hexane/ethyl acetate, 4/6, v/v).

*N-(4-(N-(5-allyl-2-hydroxy-3-methoxyphenyl)sulfamoyl)phenyl)acetamide (**4a**):* Light yellow solid; 40% yield; m.p.: 167-168 ºC. IR ($\bar{\upsilon}_{máx}$, in cm^{-1}): 3307 (N-H), 1682 (C=O), 1590, 1515 (C=C), 1311, 1152 (S=O), 1256 (C-O-C). ^{1}H-NMR (δ ppm; DMSO-d_6, 300 MHz): 10.29 (s;

1H; O<u>H</u>), 8.85 (sl; 2H; N<u>H</u>SO_2, N<u>H</u>$COCH_3$), 7.64 (s; 4H; H2', H3'), 6.57 (d; 1H; *J* = 1.8 Hz; H4), 6.53 (d; 1H; *J* = 1.7 Hz; H6), 5.87-5.78 (m; 1H; CH_2=C<u>H</u>-CH_2), 5.00-4.94 (m; 2H; C<u>H_2</u>=CH-CH_2), 3.68 (s; 3H; OC<u>H_3</u>), 3.16 (d; 2H; *J* = 6.5 Hz; CH_2=CH-C<u>H_2</u>), 2.05 (s; 3H; NHCOC<u>H_3</u>). ^{13}C-NMR (δ ppm; DMSO-d_6, 75 MHz): 169.3 (C5'), 147.8 (C3), 143.0 (C4'), 137.8 (CH_2=<u>C</u>H-CH_2), 137.5 (C1'), 134.1 (C5), 129.8 (C1), 128.1 (C2'), 124.2 (C2), 118.4 (C3'), 116.1 (C4), 115.7 (<u>C</u>H_2=CH-CH_2), 109.3 (C6), 55.9 (O<u>C</u>H_3), 39.5 (CH_2=CH-<u>C</u>H_2), 24.2 (NHCO<u>C</u>H_3). HRMS-ESI (*m/z*): calcd. for $C_{18}H_{20}N_2O_5S$ $(M+Na)^+$: 399.0991; found: 399.0985.

*N-(4-(N-(2-hydroxy-3-methoxy-5-propylphenyl)sulfamoyl)phenyl)acetamide (**4b**):* Beige solid; 25% yield; m.p.: 176-180 ºC. IR ($\bar{\upsilon}_{máx}$, in cm^{-1}): 3537, 3364 (N-H), 3154 (O-H), 2923 (C-H), 1687 (C=O), 1589, 1512 (C=C), 1312, 1158 (S=O), 1256 (C-O-C). ^{1}H-NMR (δ ppm; DMSO-d_6, 300 MHz): 10.26 (s; 1H; OH), 8.95 (s; 1H; N<u>H</u>SO_2), 8.56 (s; 1H; N<u>H</u>$COCH_3$), 7.65 (s; 4H; H2', H3'), 6.58 (d; 1H; *J* = 1.9 Hz; H4), 6.53 (d; 1H; *J* = 1.9 Hz; H6), 3.69 (s; 3H; OCH_3), 2.36 (t; 2H; *J* = 7.4 Hz; CH_3-CH_2-CH_2), 2.06 (s; 3H; NHCO<u>C</u>H_3), 1.52-1.40 (sex; 2H; CH_3-CH_2-CH_2), 0.80 (t; 3H; *J* = 7.3 Hz; CH_3-CH_2-CH_2).^{13}C-NMR (δ ppm; DMSO-d_6, 75 MHz): 169.0 (C5'), 147.6 (C3), 142.9 (C4'), 137.1 (C1'), 134.0 (C5), 132.0 (C1), 128.0 (C2'), 124.2 (C2), 118.2 (C3'), 115.8 (C4), 109.1 (C6), 55.8 (O<u>C</u>H_3), 37,0 (CH_3-CH_2-C<u>H_2</u>), 24.1 (NHCO<u>C</u>H_3), 24.1 (CH_3-C<u>H_2</u>-CH_2), 13.4 (<u>C</u>H_3-CH_2-CH_2). HRMS-ESI (*m/z*): calcd. for $C_{18}H_{22}N_2O_5S$ $(M+H)^+$: 379.1328; found: 379.1315.

*N-(4-(N-(2-allyl-5-hydroxy-4-methoxyphenyl)sulfamoyl)phenyl)acetamide (**4a'**):* Yellow solid; 43% yield; m.p.167-168 ºC. IR ($\bar{\upsilon}_{máx}$, in cm^{-1}): 3307 (N-H), 1682 (C=O), 1590, 1515 (C=C), 1311, 1152 (S=O), 1256 (C-O-C). ^{1}H-NMR (δ ppm; DMSO-d_6, 300 MHz): 10.30 (s; 1H; O<u>H</u>), 8.84 (sl; 1H; N<u>H</u>SO_2), 7.64 (s; 4H; H2', H3'), 6.57 (d; 1H; *J* = 1.9 Hz; H3), 6.53 (d; 1H; *J* = 1.8 Hz; H6), 5.86-5.75 (m; 1H; CH_2=C<u>H</u>-CH_2), 5.00-4.93 (m; 2H; C<u>H_2</u>=CH-CH_2), 3.68 (s; 3H; OC<u>H_3</u>), 3.16 (d; 2H; *J* = 6.6 Hz; CH_2=CH-C<u>H_2</u>), 2.05 (s; 3H; NHCOC<u>H_3</u>).^{13}C-NMR (δ ppm; DMSO-d_6, 75 MHz): 169.7 (C5'), 148.1 (C4'), 143.3 (C5), 138.2 (C4), 137.8 (CH_2=<u>C</u>H-CH_2), 134.4 (C1'), 130.2 (C1), 128.4 (C2'), 124.9 (C2), 118.8 (C3'), 116.4 (C3), 116.1 (<u>C</u>H_2=CH-CH_2), 109.6 (C6), 56.2 (O<u>C</u>H_3), 39.5 (CH_2=CH-<u>C</u>H_2), 24.5 (NHCO<u>C</u>H_3). HRMS-ESI (*m/z*): calcd. for $C_{18}H_{20}N_2O_5S$ $(M+H)^+$: 377.1172; found: 377.1176.

*N-(4-(N-(5-hydroxy-4-methoxy-2-propylphenyl)sulfamoyl)phenyl)acetamide (**4b'**):* Light yellow solid; 41% yield; m.p.: 176-180 ºC. IR ($\bar{\upsilon}_{máx}$, in cm^{-1}): 3536, 3362 (N-), 3143 (O-H), 1687 (C=O), 1589, 1522 (C=C), 1313, 1158 (S=O), 1255 (C-O-C). ^{1}H-NMR (δ ppm;

DMSO-d_6, 300 MHz): 10.26 (s; 1H; O<u>H</u>), 8.74 (sl; 2H; N<u>H</u>SO_2, N<u>H</u>$COCH_3$), 7.65 (s; 4H; H2', H3'), 6.58 (d; 1H; *J* = 1.7 Hz; H3), 6.53 (d; 1H; *J* = 1.7 Hz; H6), 3.69 (s; 3H; OC<u>H</u>$_3$), 2.36 (t; 2H; *J* = 7.4 Hz; CH_3-CH_2-C<u>H</u>$_2$), 2.06 (s; 3H; NHCOC<u>H</u>$_3$), 1.53-1.40 (sex; 2H; CH_3-C<u>H</u>$_2$-CH_2), 0.81 (t; 3H; *J* = 7.3 Hz; C<u>H</u>$_3$-CH_2-CH_2). ^{13}C-NMR (δ ppm; DMSO-d_6, 75 MHz): 169.0 (C5'), 147.5 (C4'), 142.9 (C5), 137.0 (C4), 133.9 (C1'), 132.0 (C1), 128.0 (C2'), 124.2 (C2), 118.2 (C3'), 115.8 (C3), 109.1 (C6), 55.7 (O<u>C</u>H_3), 36.9 (CH_3-CH_2-<u>C</u>H_2), 24.1 (NHCO<u>C</u>H_3), 24.1 (CH_3-<u>C</u>H_2-CH_2), 13.4 (<u>C</u>H_3-CH_2-CH_2). HRMS-ESI (*m/z*): calcd. for $C_{18}H_{22}N_2O_5S$ $(M+Na)^+$: 401.1147; found: 401.1128.

4.2.5 Synthesis of 4-aminobenzenesulfonamides 5a, 5b, 5a' and 5b'

Thionyl chloride (5 eq.) was added to a stirred solution of the corresponding 4-acetamidobenzene sulfonamide (1 eq.) in dry methanol (10 mL). The solution was kept under stirring at room temperature for 24 h. The progress of the reaction was monitored by TLC (chloroform/methanol, 9/1, v/v). Methanol was then removed under reduced pressure. The crude product was purified by preparative thin layer chromatography (chloroform/methanol, 9/1, v/v).

*N-(5-allyl-2-hydroxy-3-methoxyphenyl)-4-aminobenzenesulfonamide (**5a**):* Red solid; 45% yield. m.p.: 133-136 ºC. IR ($\bar{\upsilon}_{máx}$, in cm^{-1}): 3484 (N-H), 3383, 3295 (NH_2), 1622, 1594, 1515 (C=C), 1315, 1132 (S=O), 1210 (C-O-C), 1085 (C-N). ^{1}H-NMR (δ ppm; DMSO-d_6, 300 MHz): 8.63 and 8.43 (sl; 2H; N<u>H</u>$_2$), 7.38-7.33 (m; 2H; H2'), 6.62 (d; 1H; *J* = 1.9 Hz; H4), 6.52-6.50 (m; 1H; H6), 6.9-6.47 (m; 2H; H3'), 5.91 (s; 2H; O<u>H</u>, N<u>H</u>SO_2), 5.88-5.79 (m; 1H; CH_2=C<u>H</u>-CH_2), 5.02-4.96 (m; 2H; C<u>H</u>$_2$=CH-CH_2), 3.69 (s; 3H; OC<u>H</u>$_3$), 3.17 (d; 2H; *J* = 6.7 Hz; CH_2=CH-C<u>H</u>$_2$). ^{13}C-NMR (δ ppm; DMSO-d_6, 75 MHz): 152.7 (C3), 147.6 (C4'), 137.8 (CH_2=<u>C</u>H-CH_2), 136.3 (C5), 129.7 (C1), 128.8 (C2'), 125.4 (C1'), 124.9 (C2), 115.5 (<u>C</u>H_2=CH-CH_2), 114.6 (C6), 112.4 (C3'), 108.5 (C4), 55.7 (O<u>C</u>H_3), 39.7 (CH_2=CH-<u>C</u>H_2). HRMS-ESI (*m/z*): calcd. for $C_{16}H_{18}N_2O_4S$ $(M+H)^+$: 335.1066; found: 335.1060.

*4-amino-N-(2-hydroxy-3-methoxy-5-propylphenyl)benzenesulfonamide (**5b**):* Dark yellow oil; 33% yield. IR ($\bar{\upsilon}_{máx}$, in cm^{-1}): 3472 (N-H), 3375 (NH_2), 1612, 1595, 1514 (C=C), 1314, 1152 (S=O), 1215 (C-O-C), 1088 (C-N). ^{1}H-NMR (δ ppm; DMSO-d_6, 300 MHz): 8.56 and 8.39 (s; 2H; N<u>H</u>$_2$), 7.36 (d; 2H; *J* = 8.7 Hz; H2'), 6.61 (d; 1H; *J* = 1.5 Hz; H4), 6.51-6.50 (m; 1H; H6), 6.49-6.48 (m; 2H; H3'), 5.91 (s; 1H; O<u>H</u> or N<u>H</u>SO_2), 3.69 (s; 3H; OC<u>H</u>$_3$), 2.36 (t; 2H; *J* = 7.4 Hz; C<u>H</u>$_2$-CH_2-CH_3), 1.54-1.41 (m; 2H; CH_2-C<u>H</u>$_2$-CH_3), 0.82 (t; 3H; *J* = 7.3 Hz;

CH_2-CH_2-$C\underline{H}_3$).^{13}C-NMR (δ ppm; DMSO-d_6, 75 MHz): 153.7 (C3), 147.9 (C4'), 136.4 (C5), 132.5 (C1), 129.2 (C2'), 125.6 (C1'), 125.3 (C1'), 114.8 (C6), 112.8 (C3'), 108.8 (C4), 56.1 ($O\underline{C}H_3$), 37.5 ($\underline{C}H_2$-CH_2-CH_3), 24.6 (CH_2-$\underline{C}H_2$-CH_3), 13.9 (CH_2-CH_2-$\underline{C}H_3$). HRMS-ESI (*m/z*): calcd. for $C_{16}H_{20}N_2O_4S$ $(M+H)^+$: 337.1223; found: 337.1210.

*N-(2-allyl-5-hydroxy-4-methoxyphenyl)-4-aminobenzenesulfonamide (**5a'**):* Light yellow solid; 40% yield; m.p.:140-143 ºC. IR ($\bar{\upsilon}_{máx}$, in cm^{-1}): 3486 (N-H), 3383, 3294 (NH_2), 1622, 1595, 1516 (C=C), 1315, 1132 (S=O), 1210 (C-O-C), 1084 (C-N). ^{1}H-NMR (δ ppm; DMSO-d_6, 300 MHz): 8.63 and 8.43 (sl; 2H; $N\underline{H}_2$), 7.38-7.34 (m; 2H; H2'), 6.63 (d; 1H; *J* = 1.9 Hz; H3), 6.52-6.51 (m; 1H; H6), 6.50-6.47 (m; 2H; H3'), 5.91 (s; 2H; $O\underline{H}$, $N\underline{H}SO_2$), 5.88-5.79 (m; 1H; CH_2=$C\underline{H}$-CH_2), 5.02-4.96 (m; 2H; $C\underline{H}_2$=CH-CH_2), 3.69 (s; 3H; $OC\underline{H}_3$), 3.17 (d; 2H; *J* = 6.6 Hz; CH_2=CH-$C\underline{H}_2$). ^{13}C-NMR (δ ppm; DMSO-d_6, 75 MHz): 152.8 (C4'), 147.6 (C5), 137.8 (CH_2=$\underline{C}$H-CH_2), 136.3 (C4), 129.7 (C1), 128.8 (C2'), 125.4 (C1'), 124.9 (C2), 115.5 ($\underline{C}H_2$=CH-CH_2), 114.6 (C3), 112.4 (C3'), 108.5 (C6), 55.7 ($O\underline{C}H_3$), 39.7 (CH_2=CH-$\underline{C}H_2$). HRMS-ESI (*m/z*): calcd. for $C_{16}H_{18}N_2O_4S$ $(M+Na)^+$: 357.0885; found: 357.0886.

*4-amino-N-(5-hydroxy-4-methoxy-2-propylphenyl)benzenesulfonamide (**5b'**):* Dark yellow oil; 31% yield. IR ($\bar{\upsilon}_{máx}$, in cm^{-1}): 3462 (N-H), 3375, 3248 (NH_2), 1612, 1595, 1514 (C=C), 1314, 1148 (S=O), 1217 (C-O-C), 1086 (C-N).^{1}H-NMR (δ ppm; DMSO-d_6, 300 MHz): 8.56 e 8.39 (s; 2H; $N\underline{H}_2$), 7.36 (d; 2H; *J* = 8.7 Hz; H2'), 6.61 (d; 1H; *J* = 1.7 Hz; H3), 6.51-6.50 (m; 1H; H6), 6.48-6.47 (m; 2H; H3'), 5.91 (s; 1H; $O\underline{H}$ ou $N\underline{H}SO_2$), 3.69 (s; 3H; $OC\underline{H}_3$), 2.36 (t; 2H; *J* = 7.4 Hz; $C\underline{H}_2$-CH_2-CH_3), 1.53-1.41 (m; 2H; CH_2-$C\underline{H}_2$-CH_3), 0.81 (t; 3H; *J* = 7.3 Hz; CH_2-CH_2-$C\underline{H}_3$). ^{13}C-NMR (δ ppm; DMSO-d_6, 75 MHz): 152.5 (C4'), 147.2 (C5), 135.7 (C4), 131.8 (C1'), 128.6 (C2'), 124.9 (C1), 124.6 (C2), 114.1 (C3), 112.1 (C3'), 108.1 (C6), 55.5 ($O\underline{C}H_3$), 36.8 ($\underline{C}H_2$-CH_2-CH_3), 23.9 (CH_2-$\underline{C}H_2$-CH_3), 13.2 (CH_2-CH_2-$\underline{C}H_3$). HRMS-ESI (*m/z*): calcd. for $C_{16}H_{20}N_2O_4S$ $(M+H)^+$: 337.1223; found: 337.1210.

4.3 Biological assays

4.3.1 Cell lines and treatment schedule

Human tumour cell lines were used in the present study, A549 (lung carcinoma), MCF-7 (breast carcinoma), HepG2 (hepatocellular carcinoma), and HT-144 (melanoma). In addition, fibroblasts derived from human normal skin (CCD-1059Sk) and non-transformed breast epithelial cells (MCF 10A) were also examined. The cell cultures

(A549, MCF-7, HepG2, HT-144, and CCD-1059-Sk) were maintained in DMEM/F12 (Dulbecco's Modified Eagle's Minimum Essential Medium, Sigma, CA, USA) supplemented with 10% fetal bovine serum (FBS, Cultilab, São Paulo, Brazil). MCF 10A cells were cultivated in DMEM/F12 (Gibco) supplemented with 5% horse serum, 10 µg/mL insulin, 0,50 µg/mL hydrocortisone, 100 ng/mL cholera toxin and 10 ng/mL EGF. Cells were grown in a humidified atmosphere of 95% air and 5% CO_2 at 37 °C.

4.3.2 Cell viability analysis

4.3.2.1 Colorimetric assay

The cells were seeded into a 96-well plate at 5×10^4 cells/well (A549 and CCD-1059Sk) or 1×10^4 cells/well (HT-144, HepG2, MCF-7, and MCF 10A). Resazurin reduction assay was used according to the manufacturer's instructions (Sigma) to assess cell viability of A549, CCD-1059Sk, HT-144, HepG2, and MCF-7 cells. The resazurin (blue, absorption peak at 600 nm) is reduced to resorufin (pink, absorption peak at 570nm) by cell metabolically actives. Therefore, the amount of resorufin produced is directly proportional to the number of viable cells. MTT (3-(4,5-dimethylthiazol)-2,5-diphenyltetrazolium bromide) assay was used according to the manufacturer's instructions (Sigma) to assess cell viability of MCF 10A cells. The molecules were solubilized in DMSO and kept at 4 °C until use. A stock solution (20 mM) was diluted in fresh medium immediately before of the use. The substances (**4a**, **4b**, **4a'**, **4b'**, **5a**, **5b**, **5a'**, and **5b'**) were screened at 125 µM for 48 h treatment. After that, dose-response curves were performed using the most active compounds. Thus, **4b**, **4b'**, **5a**, and their precursors (sulfanilamide, eugenol, and dihydroeugenol) were tested in a concentration range of 50-400 µM for 48 h treatment on MCF-7. In these same experimental conditions, **4b**, **4b'**, and **5a** were also tested on CCD-1059-Sk and MCF 10A. The experiments were conducted in triplicate wells. IC_{50} values were determined from a non-linear regression using GraphPad Prism® (GraphPad Software, Inc., San Diego, CA, USA). Data are presented as the mean ± standard deviation (SD) of three independent experiments.

4.3.2.2 Trypan blue exclusion test

Cells were seeded into 35 mm plates at a density of 2×10^5. The treatment with compound **4b** was performed at 50 and 100 µM for 24, 48, or 72 h. Cells were harvested

with trypsin/EDTA, and trypan blue solution (0.4%) was added to the cellular suspension (1:1). Subsequently, cells were counted using a hemocytometer chamber and a light microscope. Non-viable (blue stained) and viable cells (unstained) were quantified from three independent experiments. The results are presented as mean ± SD.

4.3.3 Clonogenic assay

The clonogenic assay was performed according to Franken et al. (2006). Briefly, 100 cells were seeded into 35 mm plates. Cells were treated for 48 h with compound **4b** at 50, 100, and 200 µM and recovered in a drug-free medium for subsequent 15 days. Afterward, the colonies were fixed and stained with Crystal Violet. Only colonies with > 50 cells were counted by direct visual inspection with a stereomicroscope at 20× magnification. Assays were performed in triplicate and data were presented as mean ± SD of three independent experiments.

4.3.4 Cell cycle analysis

To analyse cell cycle progression, cells were treated for 48 h with compound **4b** at 50 and 100 µM. The cells were fixed with 75% ethanol at 4 °C overnight and then rinsed twice with cold phosphate-buffered saline (PBS). Then, the cells were resuspended in dye solution (PBS containing 30 µg/mL propidium iodide (PI) and 3 mg/mL RNAase). DNA was quantified 1 h after staining. The analysis was performed by flow cytometry (Guava easyCyte 8HT, Hayward, CA, USA). Results are presented as means ± standard deviations (SD) of three independent experiments.

4.3.5 Mitotic index determination from fluorescent cytological preparations

Cells were seeded into 35 mm Petri plates on coverslips at 2×10^5 cells/plate. After 48 h of treatment, the samples were fixed with 3.7% formaldehyde for 30 min. For α-tubulin immunolabeling, cells were permeabilized with Triton X-100 (0.5%) for 10 min. After blocking with 1% BSA, anti-α-tubulin antibody (1:100, clone DM1A, Sigma Aldrich) was incubated overnight. On the next day, secondary anti-mouse IgG-FITC antibody (1:100, Sigma Aldrich) was added to the sample and incubated for 2 h. Nuclei were stained with DAPI, and the coverslips were mounted on microscope slides using Vecta-Shield mounting medium (Vector Laboratories). Analyses were performed using a

fluorescence microscope (Nikon). Fluorescent cytological preparations were used to determine the frequency of mitosis (1,000 cells per sample were counted). The data are shown as the mean ± SD of three independent experiments.

4.3.6 Immunoblot

To analyse expression protein profile, MCF-7 cells were treated for 48 h with compound **4b** at 50 and 100 µM. Cells were homogenized in RIPA lysis buffer (150 mM NaCl, 1.0% Nonidet P-40, 0.5% deoxycholate, 0.1% SDS and 50 mM Tris pH 8.0) containing both protease and phosphatase inhibitors (Sigma). Lysates were centrifuged (10,000 × g) for 10 min at 4 °C. Supernatants were recovered, total proteins were quantified (BCA kit, Pierce Biotechnology Inc., Rockford, IL, USA) and resuspended in Laemmli sample buffer containing 62.5 mM Tris–HCl pH 6.8, 2% SDS, 10% glycerol, 5% 2-mercaptoethanol and 0.001% bromophenol blue. An aliquot of 50 µg protein was separated by SDS–PAGE (12%) and transferred (100 V, 250 mA for 2h) on to a PVDF membrane (Amersham Bioscience), blocked for 1h at 4 °C with blocking solution [5% non-fat milk in Tris-buffered saline (TBS) + 0.1% (v/v) Tween-20] to prevent nonspecific protein binding. The membrane was probed with primary antibodies: Cyclin D1 (Sigma – 1: 200), Cyclin E (Santa Cruz – 1:200) and α-tubulin (Sigma– 1:1000) overnight at 4 °C. After washing with TBS-tween (0.1%), the membrane was incubated with a secondary antibody (anti-rabbit peroxidase conjugated) for 2h at room temperature. Immunoreactive bands were visualized with the ECL Western Blotting Detection Kit (Amersham Pharmacia). A reprobing protocol was followed for detecting immunoreactive bands for different antibodies. Results were obtained from three independent experiments. The quantification of immunoreactive bands was performed using a public program (Image J).

4.3.7 Apoptosis detection by Annexin V/7-AAD

Kit Guava Nexin® (Merk Millipore, Massachusetts, EUA) was used according to manufacturer's instructions. To analyse apoptosis induction, MCF-7 cells were treated for 48 h with compound **4b** at 50 and 100 µM. Briefly, cells were collected by enzymatic digestion (Trypsin/EDTA, Sigma), centrifuged at 1,000 rpm for 5 min at 4 °C, washed with ice-cold PBS, and then 2×10^4 cells were resuspended in 100 µL of DMEM. In the next step, 100 µL of mix solution containing buffered Annexin V-PE and 7-AAD was added. The samples were read after 20 min of incubation at room temperature in a dark chamber. The

analysis was performed by flow cytometry using GuavaSoft 2.7 software. The experiments were conducted in triplicate and repeated twice. Data are presented as mean ± SD.

4.3.8 Mitochondrial integrity analysis

The integrity of mitochondria was examined by using MitoTracker Red fluorescent dye (Invitrogen, Molecular Probes, ThermoFisher Scientific) according to manufacturer's instructions. MCF-7 cells were treated for 48 h with compound **4b** at 50 and 100 µM. The cells were collected by enzymatic digestion (Trypsin/EDTA), centrifuged at 1,000 rpm for 5 min at 4 °C, washed with ice-cold PBS and incubated with MitoTracker® (500 nM) at room temperature for 45 minutes in a dark chamber. The analysis was performed by flow cytometry using GuavaSoft 2.7 software. The experiments were conducted in triplicate and repeated twice. Data are presented as mean ± SD.

4.3.9 Statistical analysis

The results were tested for significance using one-way analysis of variance (ANOVA) followed by a Tukey's post-test. The values were expressed as mean ± SD.

Conflict of interest

The authors declare no conflict of interest.

Acknowledgments

The authors are grateful to Brazilian Agencies FAPEMIG for financial support (APQ-01209-13, APQ-02810-16) and CAPES for the scholarship (H.A.B and G.A.F.S).

References

Abbot, V., Sharma, P., Dhiman, S., Noolvi, M. N., Patel, H. M., Bhardwaj, V., 2017. Small hybrid heteroaromatics: resourceful biological tools in cancer research. RSC Adv. 7, 28313–28349.

Abrão, P. H. O., Pizi, R. B., Souza, T. B., Silva, N. C., Fregnan, A. M., Silva, F. N., Coelho, L. F. L., Malaquias, L. C. C., Dias, A. L. T., Dias, D. F., Veloso, M. P., Carvalho, D. T.,

2015. Synthesis and biological evaluation of new eugenol Mannich bases as promising antifungal agents. Chem Biol Drug Des. 86, 459–465.

Ahmad, A., Khan, A., Khan, L. A., Manzoor, N., 2010. *In vitro* synergy of eugenol and methyleugenol with fluconazole against clinical *Candida* isolates. J Med Microbiol. 59 (10), 1178–1184.

Al-Sharif, I., Remmal, A., Aboussekhra, A., 2013. Eugenol triggers apoptosis in breast cancer cells through E2F1/survivin down-regulation. BMC Cancer, 13, 1–10.

Baskaran, Y., Periyasamy, V., Venkatraman, A. C., 2010. Investigation of antioxidant, anti-inflammatory and DNA-protective properties of eugenol in thioacetamide-induced liver injury in rats. Toxicology 268 (3), 204–212.

Bellamy, F. D; Ou, K., 1984. Selective reduction of aromatic nitro compounds with stannous chloride in non-acidic and non-aqueous medium. Tetrahedron Letters 25 (8), 839–842.

Boyd, A. E., 1988. Sulfonylurea receptors, ion channels, and fruit flies. Diabetes 37 (7), 847–850.

Canales, L., Bandyopadhyay, D., Banik, B. K., 2011. Bismuth nitrate pentahydrate-induced novel nitration of eugenol. Org Med Chem Lett. 1 (1), 1–3.

Carrasco, H., Raimondi, M., Svetaz, L., Liberto, M. D., Rodriguez, M. V., Espinoza, L., Madrid, A., Zacchino, S., 2012. Antifungal activity of eugenol analogues. Influence of different substituents and studies on mechanism of action. Molecules, 17 (1), 1002–1024.

Chen, Q-H., Rao, P. N. P., Knaus, E. E., 2005. Design, synthesis, and biological evaluation of *N*-acetyl-2-carboxybenzenesulfonamides: a novel class of cyclooxygenase-2 (COX-2) inhibitors. Bioorg Med Chem. 13 (7), 2459–2468.

Cortés-Rojas, D. F., Souza, C. R. F., Oliveira, W. P., 2014. Clove *(Syzygium aromaticum*): a precious spice. Asian Pac J Trop Biomed. 4 (2), 90–96.

Cottet-Rousselle C., Ronot X., Leverve X., Mayol J. F., 2011. Cytometric assessment of mitochondria using fluorescent probes. Cytometry A. 79(6):405-25.

Davis, N. M., Sokolosky, M., Stadelman, K., Abrams, S. L., Libra, M., Candido, S., Nicoletti, F., Polesel, J., Maestro, R., D'Assoro, A., Drobot, L., Rakus, D., Gizak, A.,

Laidler, P., Dulińska-Litewka, J., Basecke, J., Mijatovic, S., Maksimovic-Ivanic, D., Montalto, G., Cervello, M., Fitzgerald, T. L., Demidenko, Z. N., Martelli, A. M., Cocco, L., Steelman, L. S., McCubrey, J. A., 2014. Deregulation of the EGFR/PI3K/PTEN/Akt/mTORC1 pathway in breast cancer: possibilities for therapeutic intervention. Oncotarget 5 (13), 4603–4650.

Devi, K. P., Nisha, S. A., Sakthivel, R., Pandian, S. K., 2010. Eugenol (an essential oil of clove) acts as an antibacterial agent against *Salmonella typhi* by disrupting the cellular membrane. J Ethnopharmacol. 130 (1), 107–115.

Facchinetti, V., Moreth, M., Gomes, C. R. B., Gama, I. L., Souza, M. V. N., Pessoa, C., Rodrigues, F. A. R., Cavalcanti, B. C., Oliveira, A. C. A, Carneiro, T. R., 2014. Evaluation of (2*S*,3*R*)-2-(amino)-[4-(*N*-benzylarenesulfonamido)-3-hydroxy-1-phenylbutane derivatives: a promising class of anticancer agents. Med Chem Res. 24, 533–542.

Ferlay, J., Soerjomataram, I., Dikshit, R., Eser, S., Mathers, C., Rebelo, M., Parkin, D. M., Forman, D., Bray, F., 2015. Cancer incidence and mortality worldwide: sources, methods and major patterns in GLOBOCAN 2012. International J Cancer 136 (5), 359–386.

Fortin, S., Wei, L., Moreau, E., Lacroix, J., Côté, M-F., Petitclerc, E., Kotra, L., Lakshmi, P., Gaudreault, R. C., 2011. Substituted phenyl 4-(2-oxoimidazolidin-1-yl)benzenesulfonamides as antimitotics. Antiproliferative, antiangiogenic and antitumoral activity, and quantitative structure-activity relationships Europ J Med Chem. 46, 5327–5342.

Foster, D. A., Yellen, P., Xu, L., Saqcena, M., 2010. Regulation of G1 cell cycle progression: Distinguishing the restriction point from a nutrient-sensing cell growth checkpoint(s). Genes & Cancer 1(11), 1124–1131.

Franken, N. A. Rodermond, H. M., Stap, J., Haveman, J., van Bree, C., 2006. Clonogenic assay of cells *in vitro*. Nat Protoc. 1 (5), 2315–2319.

Ghorab, M. M., Ragab, F. A., Heiba, H. I., El-Gazzar, M. G., Zahran, S. S., 2015. Synthesis, anticancer and radiosensitizing evaluation of some novel sulfonamide derivatives. Europ J Med Chem. 92, 682–692.

Ghosh, R., Ganapathy, M., Alworth, W. L., Chan, D. C., Kumar, A. P., 2009. Combination of 2-methoxyestradiol (2-ME2) and eugenol for apoptosis induction synergistically in androgen independent prostate cancer cells. J Steroid Biochem. Mol. Biol. 113, 25–35.

Ghosh, R., Nadiminty, N., Fitzpatrick, J. E., Alworth, W. L., Slaga, T. J., Kumar, A. P., 2005. Eugenol causes melanoma growth suppression through inhibition of E2F1 transcriptional activity. J Biol Chem. 280, 5812–5819.

Hanahan, D., Weinberg, R.A., 2011. Hallmarks of Cancer: The next generation. Cell. 144 (5), 646–674.

Júnior, P. L. S., Câmara, D. A. D., Costa, A. S., Ruiz, J. L. M., Levy, D., Azevedo, R. A., Pasqualoto, K. F. M., Oliveira, C. F., Melo, T. C., Pessoa, N. D. S., Fonseca, P. M. M., Pereira, A., Araldi, R. P., Ferreira, A. K., 2016. Apoptotic effect of eugenol envolves G2/M phase abrogation accompanied by mitochondrial damage and clastogenic effect on cancer cell *in vitro.* Phytomedicine 23 (7), 725–735.

Kalmes, M., Blömeke, B., 2012. Impact of eugenol and isoeugenol on AhR translocation, target gene expression, and proliferation in human HaCat keratinocytes. J Toxicol Environ Health A. 75 (8-10), 478–491.

Kamal, A., Dastagiri, D., Ramaiah, M. J., , Reddy, J. S., Bharathi, E. V., Reddy, M. K., Sagar, M. V. P., Reddy, T. L., Pushpavalli, S. N. C. V. L., Pal-Bhadra, M., 2011. Synthesis and apoptosis inducing ability of new anilino substituted pyrimidine sulfonamides as potential anticancer agents. Europ J Med Chem. 46 (12), 5817–5824.

Kanda, Y., Kawanishi, Y., Oda, K., Sakata, T., Mihara, S., Asakura, K., Kanemasa, T., Ninomiya, M., Fujimoto, M., Konoike, T., 2001. Synthesis and structure-activity relationships of potent and orally active sulfonamide ETB selective antagonists. Bioorg Med Chem. 9 (4), 897–907.

Kim, G. C., Choi, D. S., Lim, J. S., Jeong, H. C., Kim, I. R., Lee, M. H., Park, B. S., 2006. Caspases-dependent apoptosis in human melanoma cell by eugenol. Korean J Anat. 39, 245–253.

Kim, J. K., Diehl, J. A., 2009. Nuclear cyclin D1: An oncogenic driver in human cancer. J Cell Physiol. 220(2), 292–296.

Kumari, S., Puneet, Prasad, S. B., Yadav, S. S., Kumar, M., Khanna, A., Dixit, V. K., Nath, G., Singh, S., Narayan, G., 2016. Cyclin D1 and cyclin E2 are differentially expressed in gastric cancer. Med Oncol. 33 (5), 1–10.

Kwon, Y., Song, J., Lee, H., Kim, E-Y, Lee, K., Lee, S. K., Kim, S., 2015. Design, synthesis, and biological activity of sulfonamide analogues of antofine and cryptopleurine as potent and orally active antitumor agents. J Med Chem. 58 (19), 7749–7762.

Lal, J., Gupta, S. K., Thavaselvam, D., Agarwal, D. D., 2013. Biological activity, design, synthesis and structure activity relationship of some novel derivatives of curcumin containing sulfonamides. Europ J Med Chem. 64, 579–588.

Lesch, J. E. 2007. The first miracle drugs: how the sulfa drugs transformed medicine, Oxford University Press, New York.

Li, W., Chen, H., He, Z., Han, C., Liu, S., Li, Y., 2015. Influence of surfactant and oil composition on the stability and antibacterial activity of eugenol nanoemulsions. LWT - Food Sci Technol. 62 (1), 39–47.

Malhotra, G. K., Zhao, X., Band, H., Band, V., 2010. Histological, molecular and functional subtypes of breast cancers. Cancer Biol Ther. 10 (10), 955–960.

Manikandan, P., Vinothini, G., Priyadarsini, R. V., Prathiba, D., Nagini, S., 2011. Eugenol inhibits cell proliferation via NF-κB suppression in a rat model of gastric carcinogenesis induced by MNNG. Invest. New Drugs 29, 110–117.

Matsuura, I., Denissova, N. G., Wang, G., He, D., Long, J., Liu, F., 2004. Cyclin-dependent kinases regulate the antiproliferative function of Smads. Nature 430, 226–231.

Maughan, K. L., Lutterbie, M. A., Ham, P. S., 2010. Treatment of breast cancer. Am Fam Physician 81 (11), 1339–1346.

Neff, K. M., Nawarskas, J. J., 2010. Hydrochlorothiazide versus chlorthalidone in the management of hypertension. Cardiol Rev. 18 (1), 51–56.

Parker, M. H., Smith-Swintosky, V. L., McComsey, D. F., Huang, Y., Brenneman, D., Klein, B., Malatynska, E., White, H. S., Milewski, M. E., Herbs, M., Finley, M. F. A., Liu, Y., Lubin,M. L., Qin, N., Iannucci, R., Leclercg, L., Cuyckens, F., Reitz, A. B., Maryanoff, B. E., 2009. Novel, broad-spectrum anticonvulsants containing a sulfamide group:

advancement of *N*-((benzo[b]thien-3-yl)methyl)sulfamide (JNJ-26990990) into human clinical studies. J Med Chem. 52 (23), 7528–7536.

Perou, C. M., Sørlie, T., Eisen, M. B., van de Rijn, M., Jeffrey, S. S., Rees, C. A., Pollack, J. R., Ross, D. T., Johnsen, H., Akslen, L. A., Fluge, O., Pergamenschikov, A., Williams, C., Zhu, S. X., Lønning, P. E., Børresen-Dale, A. L., Brown, P. O., Botstein, D., 2000. Molecular portraits of human breast tumours. Nature 406 (6797), 747–752.

Pisano, M., Pagnan, G., Loi, M., Mura, M. E., Tilocca, M. G., Palmieri, G., Fabbri, D., Dettori, M. A., Delogu, G., Ponzoni, M., Rozzo, C., 2007. Antiproliferative and pro-apoptotic activity of eugenol-related biphenyls on malignant melanoma cells. Mol Cancer 6, 8–20.

Prat, A., Perou, C. M., 2011. Deconstructing the molecular portraits of breast cancer. Mol Oncol. 5 (1), 5–23.

Prat, A., Pineda, E., Adamo, B., Galván, P., Fernández, A., Gaba, L., Díez, M., Viladot, M., Arance, A., Muñoz, M., 2015. Clinical implications of the intrinsic molecular subtypes of breast cancer. Breast 24 Suppl 2, S26-35.

Ross, J. S., Hatzis, C., Symmans, W. F., Pusztai, L., Hortobágyi, G N., 2008. Commercialized multigene predictors of clinical outcome for breast cancer. Oncologist 13 (5), 477–493.

Shin, S. H., Park, J. H., Kim, G. C., 2007. The mechanism of apoptosis induced by eugenol in human osteosarcoma cells. J Korean Oral Maxillofac. Surg. 33, 20–27.

Silva, C. R., Borges, F. F. V., Bernardes, A., Perez, C. N., Silva, D. M., Chen-Chen, L., 2015. Genotoxic, cytotoxic, antigenotoxic, and anticytotoxic effects of sulfonamide chalcone using the Ames Test and the mouse bone marrow micronucleus test. PLos ONE 10 (9), e0137063.

Sorlie, T., Tibshirani, R., Parker, J., Hastie, T., Marron, J. S., Nobel, A. Deng, S., Johnsen, H., Pesich, R., Geisler, S., Demeter, J., Perou, C. M., Lønning, P. E., Brown, P. O., Børresen-Dale, A. L., Botstein, D., 2003. Repeated observation of breast tumor subtypes in independent gene expression data sets. Proc Natl Acad Sci USA 100, 8418–8423.

Souza, T. B., Brito, K. M. O., Silva, N. C., Rocha, R. P., Sousa, G. F., Duarte, L. P., Coelho, L. F. L., Dias, A. L. T., Veloso, M. P., Carvalho, D. T., Dias, D. F., 2016. New eugenol glucoside-based derivative shows fungistatic and fungicidal activity against opportunistic *Candida glabrata*. Chem Biol Drug Des. 87 (1), 83–90.

Souza, T. B., Orlandi, M., Coelho, L. F. L., Malaquias, L. C. C., Dias, A. L. T., Carvalho, R. R., Silva, N. C., Carvalho, D. T., 2014. Synthesis and *in vitro* evaluation of antifungal and cytotoxic activities of eugenol glycosides. Med Chem Res. 23, 496–502.

Souza, T. B., Raimundo, P. O. B., Andrade, S. F., Hipólito, T. M. M., Silva, N. C., Dias, A. L. T., Ikegaki, M., Rocha, R. P., Coelho, L. F. L., Veloso, M. P., Carvalho, D. T., Dias, D. F., 2015. Synthesis and antimicrobial activity of 6-triazolo-6-deoxy eugenol glucosides. Carbohydrate Res. 410, 1–8.

Supuran, C. T., Innocenti, A., Mastrolorenzo, A., Scozzafava, A., 2004. Antiviral sulfonamide derivatives. Mini Rev Med Chem. 4 (2), 189–200.

Takahashi, K., Ohta, M., Shoji, Y., Kasai, M., Kunishiro, K., Miike, T., Kanda, M., Shirahase, H., 2010. Novel Acyl-CoA: cholesterol acyltransferase inhibitor: Indoline-based sulfamide derivatives with low lipophilicity and protein binding ratio. Chem Pharmac Bulletin 58 (8), 1057–1065.

Torre, L. A., Siegel, R. L., Ward, E. M., Jemal, A., 2016. Global cancer incidence and mortality rates and trends - An Update. Cancer Epidemiol Biomarkers Prev. 25 (1), 16–27.

Viegas-Junior, C., Danuello, A., Bolzani, V. S., Barreiro, E. J., Fraga, C . A. M., 2007. Molecular Hybridization: A useful tool in the design of new drug prototypes Current Med Chem. 14 (17), 1829–1852.

Wainwright, M., Kristiansen, J. E., 2011. On the 75th anniversary of Prontosil. Dyes and Pigments 88, 231–234.

Wang, G-B., Wang, L-F., Li, C-Z., Sun, J., Zhou, G-M., Yang, D-C., 2012. A facile and efficient method for the selective deacylation of *N*-arylacetamides and 2-chloro-*N*-arylacetamides catalyzed by $SOCl_2$. Res Chem Intermed. 38, 77–89.

Wang, X., Wan, K., Zhou, C., 2010. Synthesis of novel sulfanilamide-derived 1,2,3-triazoles and their evaluation for antibacterial and antifungal activities. Europ J Med Chem. 45 (10) 4631–4639.

Weir, G. M., Liwski, R. S., Mansour, M., 2011. Immune modulation by chemotherapy or immunotherapy to enhance cancer vaccines. Cancers 3 (3), 3114–3142.

Yang, M., Jiang, P., Hoffman, R. M., 2015. Early reporting of apoptosis by real-time imaging of cancer cells labeled with green fluorescent protein in the nucleus and red fluorescent protein in the cytoplasm. Anticancer Research 35, 2539–2544.

Yoo, C-B., Han, K-T., Cho, K-S., Ha, J., Park, H-J., Nam, J-H., Kil, U-H, Lee, K-T., 2005. Eugenol isolated from the essential oil of *Eugenia caryophyllata* induces a reactive oxygen species-mediated apoptosis in HL-60 human promyelocytic leukemia cells. Cancer Lett. 225 (1), 41–52.

Zolfigol, M. A., Ghaemi, E., Madrakian, E., 2001. Nitration of phenols under mild and heterogeneous conditions. Molecules 6 (7), 614–620.

Highlights

- Phenylpropanoid-based sulfonamide inhibits cell cycle progression of MCF-7 cells.
- Phenylpropanoid-based sulfonamide promotes cyclin D and E down-regulation in MCF-7 cells.
- Phenylpropanoid-based sulfonamide has pro-apoptotic activity on MCF-7 cells.